FIRST STEP IN PHYSICAL TREATMENT OF THE COLLINEAR CLUSTER TRI-PARTITION MECHANISM

Yu.V. Pyatkov[1,2], D.V. Kamanin[1], W. von Oertzen[3], A.A. Alexandrov[1], I.A. Alexandrova[1], N.A. Kondtayev[1], E.A. Kuznetsova[1], O.V. Strekalovsky[1], V.E. Zhuchko[1]

[1]Joint Institute for Nuclear Research, Dubna, Russia
[2] National Nuclear Research University "MEPHI", Moscow, Russia
[3]Helmholz–Zentrum Berlin, Berlin, Germany

INTRODUCTION

In our recent publications [1–3] we have summarized experimental evidences of the existence of a new type of the ternary decay of heavy low excited nuclei that were discovered and named by us collinear cluster tri-partition (CCT). The results obtained have inspired the series of theoretical woks dedicated to the CCT process [4–7]. The theoretical predictions put forward are based on the comparison of the energy "prices" of different pre-scission nuclear configurations leading to the ternary decay. The possible kinetic energies of all decay partners are estimated as well in ref. [3].

Bearing in mind that all the predictions are strongly model dependent, we have compared them with our experimental results to choose the most realistic ones. We have discussed our own scenarios of some of the CCT modes.

EXPERIMENTAL DATA

In this paper we discuss the results obtained in the experiment Ex3 performed with the COMETA setup [3]. Fig. 1*a* shows the region of the mass-mass distribution for the fission fragments (FF) from ^{252}Cf (sf) around the CCT "bump", while no additional gates on the experimental data were applied. Since the timing signals from the PIN diodes were used as the "stop" detectors this plot is almost free of the background events due to the scattering of the FF. The later allows to observe an internal structure of the "bump" consisting of the lines along $M_{1,2}$ = const (marked by the numbers 1–3). The lines marked by the arrows 2 and 3 are clearly distinguished as the peaks in the projection of the plot to M_1 axis shown in fig. 1*b*. One can also see two tilted diagonal lines along $Ms = M_1 + M_2 = 196$ amu and $Ms = 202$ amu (marked by number 4) which start from the partitions 68/128 and 68/134, respectively.

Actually, only two fragments were detected in each decay event. The mass and velocity of a "missed" fragment were calculated basing on the mass and momentum conservation laws. Fig. 2*a* demonstrates the correlation between the velocities of the two lighter partners of the ternary decay. For the sake of convenience, the FFs from ternary events are labeled by numbers 1÷3 in decreasing sequence of their masses. Three different groups of the events are vividly seen in the figure. They are marked by the signs *w*1–*w*3, respectively. We will analyze the events in each group separately. The energy spectrum of the detected Ni ions is shown in fig. 2*b*. Their yield does not exceed 10^{-4} per binary fission.

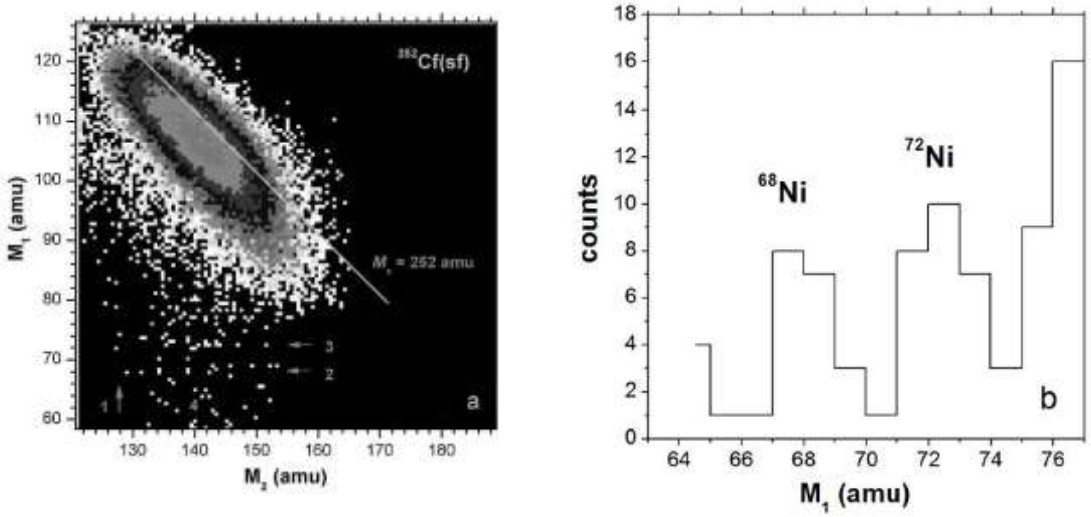

FIGURE 1. a) The region of the initial mass-mass distribution of the FFs around the CCT bump (see text for the details). b) The lines marked by the arrows 2 and 3 are shown as a projection.

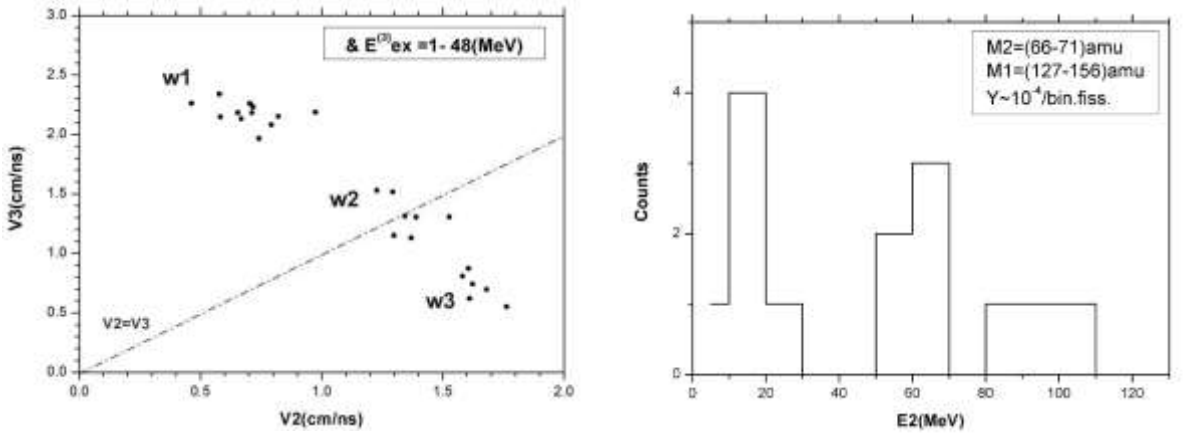

a b

FIGURE 2. a) The velocities for the lightest (*V*3) *vs* middle-mass (*V*2) fragments from the ternary decay. b) The energy spectrum of the Ni fragments from the events of the group *w2* in fig. 1a.

POSSIBLE PHYSICAL SCENARIOS FOR THE EVENTS BASED ON NI CLUSTERS

The basic properties of the events joined into *w*1–group are presented in fig. 3*a*. The respective possible scenarios of the decay standing behind are illustrated by fig. 3*b, c*.

Comparing the velocities of the decay partners for typical event from the group *w*1 one can suppose that the pre-scission configuration looks as shown in fig. 3*a*. Really, $V_1 \sim V_{H\_bin}$ where V_{H_bin} is a typical velocity of the heavy fragment in conventional binary fission. It means that the first rupture took place between ^{142}Cs and di-nuclear system ^{42}P/^{68}Ni. The charges of the FFs were calculated in the frame of the unchanged charge density hypothesis ("Z_{ucd} hypothesis"), except of ^{68}Ni which nucleon composition is due to the neutron subshell N = 40 [8]. The second rupture should happen apparently after full acceleration of the di-nuclear system ^{42}P/^{68}Ni because $V_3 > V_2$. At the same time the pre-scission configuration

contradicts to the energy conservation law. Interaction energy E_{int} between the nuclei in the chain ^{42}P/^{68}Ni/^{142}Cs (taking into account both Coulomb and nuclear components), which converts into the total kinetic energy after scissions, exceeds Q_3–value. It means that the decay according to the proposed scenario could take place due to the tunneling only. The deformation (elongation) of the decay partners could decrees the Coulomb energy but some part of the free energy must be paid as the deformation energy in this case. The following alternative scenario seems to be more realistic (fig. 3*b*).

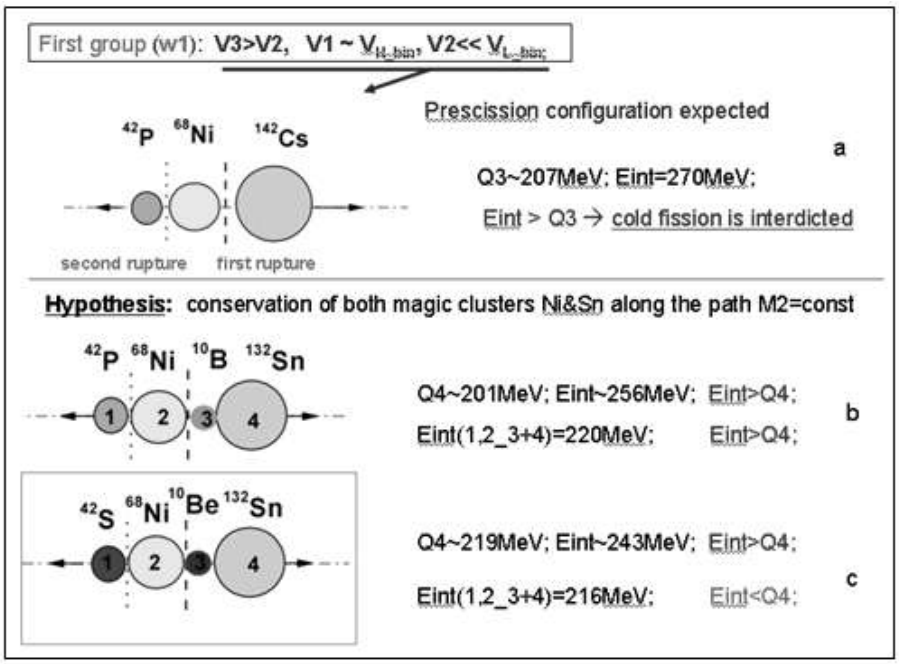

FIGURE 3. a) An example of the event from the group *w*1. b) The possible pre-scission configuration for this event under condition that nucleon composition of the light partner follows an unchanged charge density hypothesis. c) The similar configuration for the best Q4-value.

As it can be inferred from fig. 1*a* the rectangular structures appear due to both heavy and light magic clusters and they manifest themselves in the same way. Indeed, one observes both the line M_1 = const and M_2 = const. It is reasonable to suppose that both magic clusters are preformed at least at the scission configuration. It means that it can look like a chain of nuclei shown in fig. 3*b*. But it appears that $Q_4 > E_{int}$ as it was in the previous case. Supposing that the partners 3 and 4 (fig. 3*b*) move after first rupture as a single di-nuclear system we can decrease energy deficit, but still E_{int} (1, 2_3 + 4) > Q_4. At last changing nucleon composition of two lighter nuclei in order to maximize Q_4 value one succeeds to meet energy conservation law (fig. 3c).

Similar consideration was performed for the events from group *w*2 (fig. 4). The closeness of the velocities $V_3 \sim V_2$ can be explained by the specific "dynamical blocking" mechanism. We mean the following scenario. The first rupture occurred between heavy nucleus of ^{143} Cs and di-nuclear system of ^{70}Ni/^{39}P. Immediately after that the second rupture making ^{142}Cs nucleus free took place (fig. 4*a*). The nucleus of ^{39}P being lighter than the ^{70}Ni nucleus will run down it very soon but cannot outrun because the path is blocked ("dynamical blocking"). Cinematically for the Cs nucleus both nuclei move as a single system. The strong support for such scenario follows from the fact that $M_{1exp} \sim M_{1TT}$, where M_{1exp} – is the actually measured

mass of heavy fragment (using "*V–E*" method) while M_{1TT} – is the mass calculated for binary fission approach (i.e. in the frame of the "TOF–TOF" method). The proposed scenario explains the observed velocity correlations but contradicts to the energy conservation law ($E_{int} > Q_3$), i.e. cold fission via compact ternary configuration is interdicted (except tunneling provided low probability of the decay).

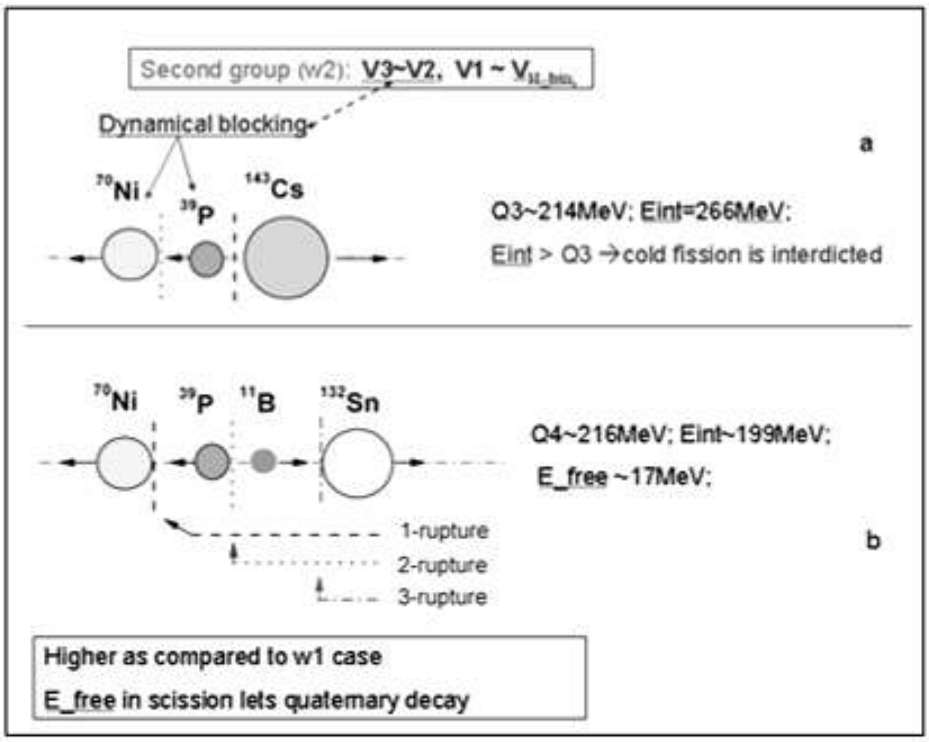

FIGURE 4. a) The parameters of the events from the group *w*2 b) The possible pre-scission configuration for these events.

Basing on the same arguments as in the previous case we suppose an elongated pre-scission configuration consisting of four nuclei (fig. 4*b*). A relatively long distance between Ni and Sn nuclei decreases total Coulomb energy while E_{int} estimated for the sequence of ruptures shown in fig. 4*b* becomes less than Q_4 even without maximizing of the latter by variation of the nucleon composition of lighter decay partners. Thus quaternary decay is expected.

The events from group *w*3 were analyzed in the same manner as those from two previous groups. Corresponding illustrations are presented in fig. 5. Once more $V_1 \sim V_{H\_bin}$ is observed while $V_3 < V_2$. In order to reproduce the experimental velocity correlations the first rupture is supposed to occur between heavy Cs nucleus and di-nuclear system of Ni/P. After full acceleration this system decays making free both constituents. The compact ternary configuration provides the expected total kinetic energy which is too high and exceeds Q_3-value (fig. 5*a*).

Decay via elongated configuration shown in fig. 5*b* overcomes this difficult. The sequence of ruptures different from the scenario for *w*2–group changes the velocity of ^{39}P nucleus (the di-nuclear system Ni/P decays on-the-fly). It is important to note that the quaternary decay channel is also predicted in the frame of the proposed scenario.

Thus the almost similar nuclear composition but a different sequence of partners and rupture scenarios is actually realized giving rise to the different kinematics of the partners involved.

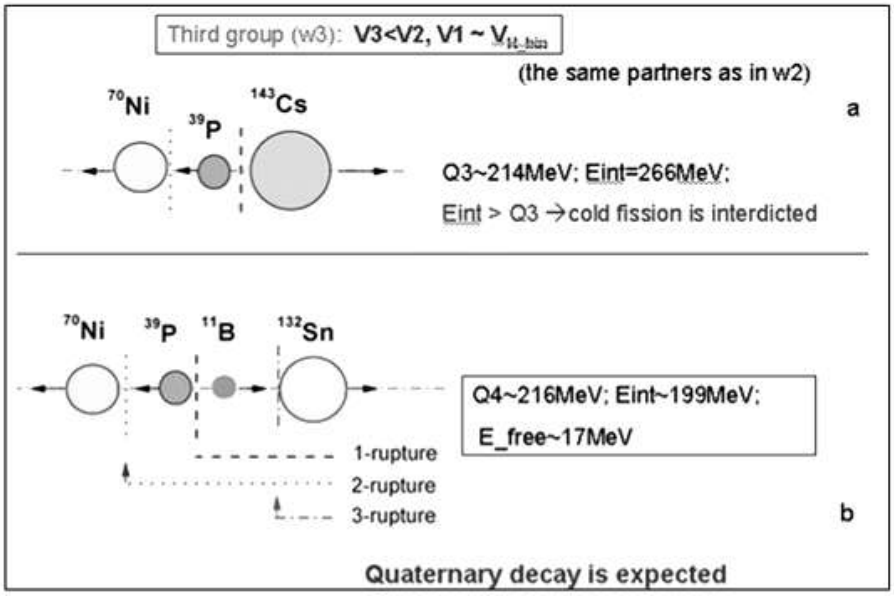

FIGURE 5. a) The parameters of the events from group *w*3. b) The possible pre-scission configuration for these events.

POSSIBLE PHYSICAL SCENARIO FOR THE EVENTS FORMING TILTED RIDGES

We come to the analysis of the structures which look like the tilted ridges in fig. 1*a*. Along each ridge the total mass of two fragments is conserved, i.e. $M_1 + M_2 = \text{const}$, that means also the mass conservation for the missed fragment ($M_3 = \text{const}$). The expected decay scenario for the events is illustrated by fig. 6.

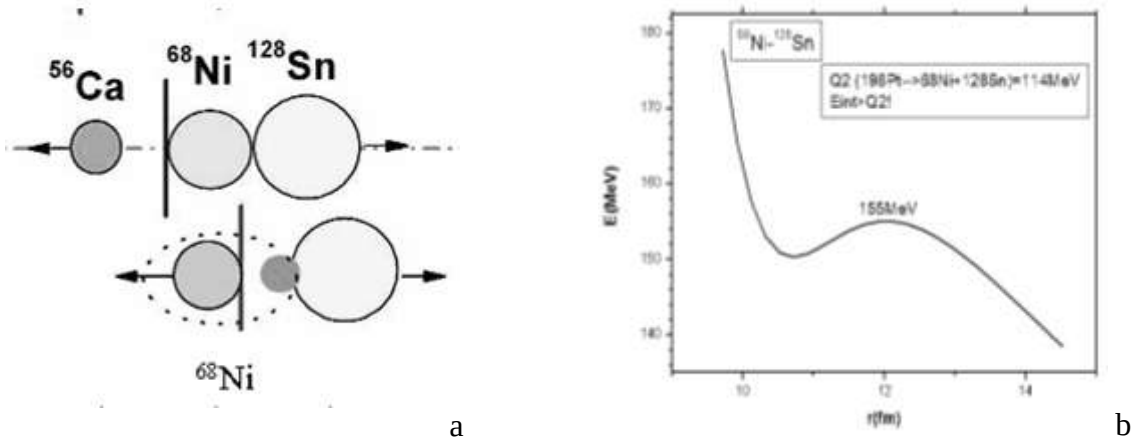

a b

FIGURE 6. a) A two-stage decay process giving rise presumably to one of the tilted ridges in fig. 1*a* ; b) The interaction potential between the fragments at the second stage of the decay.

The most left tilted ridge in the figure starts from the partition ^{68}Ni/^{128}Sn. It means that ^{56}Ca nucleus is missed in this point (the upper scheme in fig. 6*a*) and along the whole ridge as well. If one moves along the ridge the mass of the detected light fragment decreases while the heavy fragment becomes more and more heavy "nipping off" the nucleons from the Ni cluster. Fig. 6*b* gives an idea why it happens. The potential energy of the di-nuclear system ^{68}Ni/^{128}Sn is higher than *Q*–value for the decay ^{196}Pt → ^{68}Ni + ^{128}Sn. The decay of Pt nucleus can happen from a more elongated shape only. The elongation of the ^{68}Ni cluster, which must be softer than magic nucleus of ^{128}Sn, is most likely to realize via its clusterization. The process is very similar to that, which is known as the Ikeda rule [9] for the light nuclei.

COMPARISON OF THE RESULTS WITH MODEL CALCULATIONS

For the moment, there are at least two theoretical works that are known to be dedicated to the kinematical parameters of the decay partners of the collinear ternary decay [5, 6]. Only one CCT combination, namely Sn-Ca-Ni, is analyzed in the frame of a simplified model in ref. [5]. Nevertheless, a principal peculiarity of the energy spectra of the light CCT partners is reproduced, namely their two-component composition (low energy and high energy peaks). Our data from groups *w*1 and *w*2 are shown in fig. 7. The energies were estimated for three body pre-scission configurations basing on the total E_{int} and momentum conservation in a two-step sequential process. The upper high energy group of the events corresponds to the pre-scission configuration shown in fig. 3*a*. The similar calculations for the configuration from fig. 4*a* reproduce the low energy group in fig. 7. Our results agree with the predictions of the work [5] even quantitatively. But as we have shown above such decays could proceed via tunneling only. A rather similar approach was used in [6].

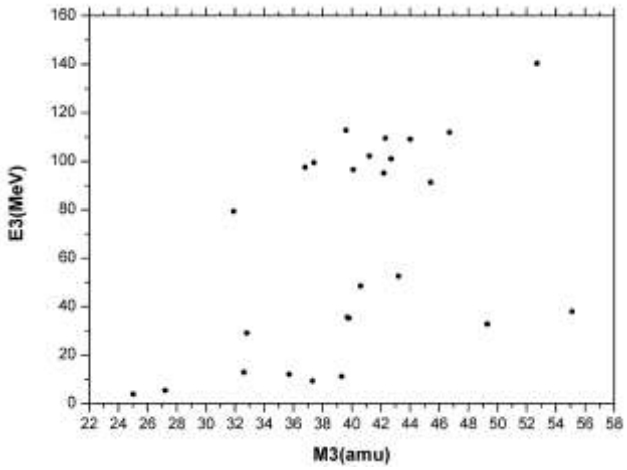

FIGURE 7. The masses and energies of the lightest CCT partner. The energies were estimated for three body pre-scission configuration. See text for details

CONCLUSIONS

1. Strong energy restrictions rule the CCT process that results in variety of exit kinematical parameters of the CCT partners in dependence of their pre-scission configuration and time scenario of the ruptures.
2. More consistent theoretical models are needed for a realistic description of the CCT process.

REFERENCES

1. Yu.V. Pyatkov et al., Eur. Phys. J. A. 2010. V. 45. P. 29–37.
2. Yu.V. Pyatkov et al., Bulletin of the Russian Academy of Sciences. Physics. 2011. V. 75. P. 949–952.
3. Yu.V. Pyatkov et al., Eur. Phys. J. A. 2012. V. 48. P. 94–109.
4. K.R. Vijayaraghavan et al., Eur. Phys. J. A. 2012. V. 48. P. 27–34.
5. R.B. Tashkhodjaev et al., Eur. Phys. J. A. 2011. V. 47. P. 136–145.
6. K. Manimaran et al., Eur. Phys. J. A. 2010. V. 45. P. 293–300.
7. V. Pashkevich et al., Int. Journal of Modern Physics E. 2010. V. 19. P. 718–724.
8. D. Rochman et al., Nucl. Phys. A. 2004. V. 735. P. 3–20.
9. H. Horiuchi, K. Ikeda, Cluster Model of the Nucleus. Int. Rev of Nucl. Phys. Eds. T. T. S. Kuo and E. Osnes. Vol. 4. (World Scientific, Singapore, 1986). P. 1–258.